Journal of Applied Electrochemistry (2006) 36:691–701
DOI 10.1007/s10800-006-9130-2

Effect of nickel on copper anode passivation in a copper sulfate solution by electrochemical impedance spectroscopy

G. JARJOURA and G.J. KIPOUROS*
*Materials Engineering Programme, Dalhousie University, P.O. Box 1000, Halifax, NS, B3J 2X4, Canada (*author for correspondence, e-mail: Georges.kipouros@dal.ca)*

Received 5 June 2005; accepted in revised form 23 January 2006

Key words: anode passivation, copper, diffusion coefficient, electrorefining, electrochemical Impedance Spectroscopy, surface oxides

Abstract

Electrochemical Impedance Spectroscopy (EIS) was applied on Cu–Ni samples passivated in a specially designed flat electrochemical cell which was heated at 60 °C. The electrolyte consisted of 160 g $l^{-1}H_2SO_4$, 40 g l^{-1} Cu^{2+} and 0, 10, 20, 30 or 40 g l^{-1} Ni^{2+} and the copper anodes contained nickel ranging from 0 w% to 10 w%. The oxygen content of the anodes and the electrolyte was also measured. An AC excitation signal of 10 mV and of 1mHz–100 MHz frequency was applied at the open circuit potential as well as at a passivation potential, the latter having been determined previously. The results indicate that nickel ion additions to the electrolyte increased the resistance of the electrolyte and altered the porosity, thickness and constituents of the passivation layer formed. The equivalent circuit models generated from the data acquired during the EIS experiments and the values for the electrical components were in the predicted range. The results are supported by supplementary XRD and SEM findings.

1. Introduction

High purity copper is produced by electrorefining of copper anodes containing at least 99.5% copper which are cast from fire refined blister copper [1]. Copper ions dissolve at the anode, enter the electrolyte and then selectively deposit onto the cathode under the force of an applied direct current. Impurities in the anode either dissolve into the electrolyte and circulate with it or remain at the anode and become part of the anode slimes. Among the impurities are also precious metals the recovery of which contribute into the financial success of the operation. Nickel in the anode in concentrations less than 3000 ppm dissolves virtually 100% into the electrolyte whereas in excess of that amount result in the formation of some NiO upon the solidification of the anode. Nickel oxide being a refractory, does not dissolve in the electrolyte and remains in the anode slimes. The slimes will either settle to the bottom of the cell or circulate with the electrolyte or remain attached to the copper anode forming a relatively thick porous layer of impurities. The slimes layer adds to the resistance of the diffusion layer and may contribute to the effect known as anode passivation i.e. a sharp increase in anode potential while the current applied is unchanged. During anode passivation further dissolution of the anode ceases, the electrorefining process is prematurely terminated and the remaining undissolved anode is removed and remelted. To avoid passivation the applied current density is limited to around 30 mA cm^{-2} [1].

The interpretation of the mechanism by which the anode is passivated is still an issue of disagreement. Some researchers [2] have attributed the anode passivation to the low solubility of copper sulphate in the electrolyte that causes precipitation of copper sulfate crystals at the copper anode, which in turn is insulated and the passage of current through the electrochemical cell is prevented. Other researchers [3] have postulated that passivation is due to the formation of a cuprous oxide film on the anode, formed by the following reactions:

Dissolution Reactions

$$Cu \rightarrow Cu^{+} + e^{-}(\text{fast}) \quad (1)$$

$$Cu^{+} \rightarrow Cu^{2+} + e^{-}(\text{slow}) \quad (2)$$

Passivation Reactions

$$2Cu^{+} + H_2O \rightarrow Cu_2O + 2H^{+} \quad (3)$$

$$2Cu + H_2O \rightarrow Cu_2O + 2H^{+} + 2e^{-} \quad (4)$$

According to this theory high current densities result in the build up of Cu^{+} ions at the anode surface by reaction (1) since its conversion to Cu^{2+} by reaction (2)

is slow. The cuprous ion then reacts with water, as shown in equation (3), in the electrolyte to form a cuprous oxide passivation layer. However, excessive use of supporting electrolyte (i.e. H_2SO_4), as is the industrial practice, will cause reactions (3) and (4) to shift to the left, thus minimizing passivation [3–5].

As copper refining is a primarily mass transport limited process copper ions must not only diffuse through the electrochemical diffusion layer at the anode surface but also through a slime layer that builds up on copper anode as it dissolves.

In a stationary vertical copper electrode the increase in the current density and the addition of H_2SO_4 was found to lead to precipitation of $CuSO_4$ [6, 7]. In industrial practice not only the concentration of the bulk electrolyte is chosen such as to prevent a cathode-limiting situation but also the electrolyte circulation is such to avoid contamination of the final product. As the quality of the copper ores deteriorates the amount of nickel in the ore and subsequently in the electrolyte increases. The physicochemical properties of electrolytes that contain substantial amounts of nickel ions have been studied [8, 9]. Several recent studies, using linear sweep voltammetry and chronopotentiometry, have been done to determine the influence of impurities, in the copper anodes as well as the electrolyte, on copper passivation [10–13]. None of these studies were done on copper samples alloyed individually with nickel. Also 3-electrode techniques were applied involving the rotating disc electrode (RDE), linear sweep voltammetry (LSV), chronopotentiometry (CP), and cyclic voltammetry. (CV) on unrefined copper anodes and synthetic copper/nickel alloys in a synthetic electrolyte containing 160 g l^{-1} sulphuric acid, 40 g l^{-1} Cu^{2+} and nickel ion concentrations ranging from 0 to 40 g l^{-1} [14].

The purpose of the present research was to apply electrochemical impedance spectroscopy (EIS) on unrefined and synthetic copper/nickel alloy samples that contained nickel and passivated in a synthetic electrolyte containing 160 g l^{-1} sulphuric acid, 40 g l^{-1} Cu^{2+} and nickel ion concentrations ranging from 0 to 40 g l^{-1} at a temperature 60 °C. The surface oxide layers were characterized using X-ray diffraction (XRD) and scanning electron spectroscopy (SEM).

2. Experimental

2.1. *Materials*

Pure copper (99.999%) sheets and cast copper (99%) were available from previous work in the laboratory [9]. Samples of unrefined commercial copper anodes were prepared by re-melting pieces of real operation size commercial anodes [8] in an induction furnace, under an argon atmosphere in cylindrical boron nitride crucibles of 1.3 cm inner diameter. They were then cooled slowly under the same atmosphere and transferred to a tube furnace where they were homogenized for 10 h at a temperature of 950 °C, under an argon atmosphere. The finished samples were cut into 10 pieces 1 cm in thickness each. Chemical analysis was performed using Atomic Absorption Spectrometry (Varian SpectrAA model 55B). The chemical synthesis of the commercial unrefined copper anode is shown in Table 1. The error of determination is ±1%. It can be seen that the commercial unrefined copper anode contains most of the impurities which were mentioned previously.

For the 3-electrode electrochemical experiments a 2 cm^2 circular piece electrode was prepared by melting oxygen free copper and ultra pure nickel in cylindrical boron nitride crucibles in the same induction furnace mentioned earlier, under an argon/7 volume% hydrogen atmosphere. The samples were kept in the molten state for about 30 min to insure complete melting of all the constituents of the alloys and the removal of as much of the oxygen that might be present. They were then cooled slowly to avoid the formation of any cavities due to rapid shrinkage. The samples were then transferred to a tube furnace where they were homogenized under an argon/7 volume % hydrogen atmosphere, for 10 h at a temperature of 1000 °C. Finished samples were cut into 10 pieces 1 cm in thickness. The nickel content of the synthetic copper-nickel anodes was determined using Atomic Absorption Spectrometry. The estimated error was 1 to 2% of amount present.

The compositions of these electrodes are listed in Table 2. The oxygen content was determined by a carbothermal reduction analysis (LECO TC-436) a method developed previously [15]. Samples for carbothermal reduction analysis were prepared immediately after sampling. The samples being 0.1–0.2 g each were transferred into pre-weighted adding a pair of tweezers. The tin-capsules were closed tight, the weight determined and put into numbered glass containers with plastic caps. The samples for analysis were transferred to the LECO instrument, and analysis performed immediately to avoid exposure of the metal in the tin-capsules to air. In addition, the samples were examined by SEM to determine whether the oxygen is present as NiO or as solid solution.

The counter electrode for the electrochemical processes was a 316L stainless steel bar measuring 0.5 cm in diameter and 10 cm in length whereas Ag/AgCI (in 1 M KCl) equipped with a Luggin capillary was used as a reference electrode.

Table 1. Chemical analysis of unrefined commercial copper anodes

Element	Si	Bi	Te	Sb	As	Ni	O	Fe	Au	Pb	Cu
Amount/ppm (%)	115	133	54	181	925	3800	–	2300	2.1	124	–

Table 2. Composition of the synthetic copper electrodes

Sample ID	Ni/ w%	O/ppm
CN0	0	15
CN1	1	10
CN2	2	15
CN3	3	11
CN4	4	13
CN5	5	7
CN6	6	41
CN8	8	19
CN9	9	53
CN10	10	4

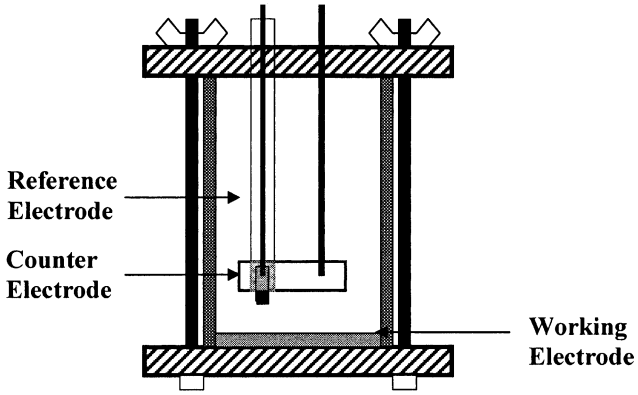

Fig. 1. Flat cell for EIS experiments.

2.2. *Electrolyte*

Synthetic electrolytes were prepared from laboratory grade chemicals dissolved in 18 MΩ cm deionized water. Concentrated sulphuric acid (98%), hydrated copper sulphate $CuSO_4 \cdot 5H_2O$ and hydrated nickel sulphate $NiSO_4 \cdot 6H_2O$ were used as source chemicals. During the experiments, the electrolyte was kept at a temperature of 60 °C to simulate industrial environments. The oxygen content in the electrolyte for all the experiments was monitored using an oxygen meter. The meter was calibrated before each measurement using a wet towel to provide a 100% humidity environment and the numbers were adjusted according to calibration tables provided by the manufacturer.

2.3. *Electrochemical cell and instrumentation*

All electrochemical experiments were performed at a controlled electrolyte temperature using a Dyna-Sense thermoregulator control system, composed of a variable output controller and a mercury thermoregulator that has a maximum sensitivity of 0.003 °C. The flat cell designed for optimum current distribution and shown in Figure 1 was used for the electrochemical impedance spectroscopy (EIS) experiments. The flat cell consisted of a cylindrical body made of Plexiglas with an O-ring grooved bottom edge for direct clamping to a flat sample. The counter electrode, made of Pt expanded mesh with an area of about 3.5 cm^2, parallel to the surface of the sample to provide optimum current distribution for EIS measurements. An Ag/AgCI reference electrode (in 1 M KCl) was mounted so as to fit through an opening in the counter electrode. The cell body rested on the sample and was pressure clamped to the sample between the top and bottom plates with four threaded stainless steel rods.

An EG&G model 273A potentiostat controlled by Labview™ software was used to perform the EIS tests. The potentiostat was calibrated by EG&G, and was checked for any drift from calibration on a weekly basis using a dummy cell. The potentiostat is connected to the electrochemical cell by means of an electrometer, which measures the potential difference between the reference and working electrodes. A Fluke 45 dual display multimeter was used to check if the values displayed by the potentiostat and the FRA were correct. The multimeter was calibrated using a Fluke 9100 Universal Calibration System to insure proper operation and accurate readings. Instrumental control, data acquisition, and processing were performed by an in-house driver for national instrument LabView™.

A Solartron 1255 Frequency. Response Analyzer (FRA), controlled by a Scribner Associates Electrochemical Impedance Spectroscopy, Zplot, was used for the Electrochemical Impedance Spectroscopy measurements. The FRA consists of a sweep generator to generate sine waves at a given frequency, a voltmeter, and a phase meter. In a typical experiment, two channels on the FRA were used, one to measure the potential at a specified frequency, and the other to record the resulting current at that frequency. The ratio of the two channels is the impedance. The potential and the phase were found accurately using a digital Fourier integration. Once measurements at a given frequency are done, the RFA moves automatically to the next frequency and the same measurements are performed. The RFA was calibrated and was checked for any drift from calibration using an in-house built dummy cell.

2.4. *Characterization equipment*

A Hitachi S-4700 Field Emission Scanning Electron Microscope (FESEM) operating at 2 kV and a current of 50 μA was used to study the surface morphology of specific samples. The passive layers were characterized using an Oxford INCA Energy 200 EDS System, equipped with a 30 mm^2 Si(Li) crystal, 136 eV resolution at Mn Ka, SATM window covering from B to U detection. This facility provided rapid, non-destructive, and quantitative chemical analyses of the surface of the samples.

X-ray diffraction was done using a Siemens D5000 X-Ray Diffractometer equipped with a copper X-Ray tube and a scintillation counter. To accomplish phase identification the peaks and relative intensities from the specimen are compared with peaks and relative intensities from a very large set of standard data, both experimental and calculated.

3. Experimental Procedure

Copper/ nickel samples of composition 0, 1, 2, 3, 4, 5, 6, 7, 8, 9 and 10% Ni and unrefined commercial anodes were used as anodes, and stainless steel rods were used as cathodes. The cell electrolyte consisted of 160 g l^{-1} H_2SO_4, 40 g l^{-1} Cu^{2+} and 0, 10, 20, 30 or 40 g l^{-1} Ni^{2+}. The cell assembly was heated to 60 °C and maintained at that temperature throughout the experiment with the aid of an electrical tape and a temperature controller. Prior to each experiment, the anodes were subjected to two stages of wet polishing using 1 and 0.05μm alumina, washed with deionized distilled water first and then with methanol. After the samples were completely dry they were mounted in the flat cell which exposes 1 cm^2 of the sample to the test solution. The electrolyte was flushed with argon, and a blanket of the same gas was kept over the solution.

During a typical experiment the AC excitation signal of 10 mV and of 1 mHz–100 MHz frequency was applied at the open circuit potential as well as at a passivation potential [14]. The FRA collected and recorded the real and imaginary components of the impedance response of the system.

All data were plotted vs frequency and then analyzed and fitted into equivalent circuits. The response of the system was analyzed and the results are plotted in terms of the Nyquist and Bode plots. On the Nyquist plot, in the low frequency region, the Warburg resistance could be attributed to diffusional processes either in the electrolyte or through the passivation layer on the surface of the anode. It could be also attributed to reactions taking place on the passivation layer. In this study the low frequency region has not been observed due to the extreme noisy conditions.

4. Results and Discussion

Figure 2 shows a plot of the imaginary impedance component (Z'') against the real impedance component (Z') at each excitation frequency for a pure copper anode in an electrolyte containing, 160 g l^{-1} H_2SO_4, 40 g l^{-1} $CuSO_4$ and 0, 10, 20, 30, or 40 g l^{-1} $NiSO_4$. The segment MN in the low frequency region of the Nyquist plot could be the beginning of a large semi-circle which could be attributed to the capacitance of a second layer that formed or precipitated on the surface of the anode. Alternatively, it could also be attributed to adsorption of ions onto the surface of the anode. The presence of the depressed semi circle (LM) in the high frequency region of the Nyquist plot could be due to the capacitance of the double layer, or to high rate reactions taking place on the surface of the anode. The center of the semi circle (MN) does not lie on the real axis. This is due to the geometry of the anode, which includes surface roughness, porosity, and inhomogeneity. In some cases, such as curves D and E, an inverted loop appears which could be attributed to the formation of a second phase in the layer that was represented by segment MN. The resistance of the electrolyte is the point were the curve representing each electrolyte composition intersects the Z' axis. As the nickel ion concentration in the electrolyte increased so did the resistance of the electrolyte, in agreement with previous findings [9]. Inductive behaviour shown at the end of the high frequency loops may be due to equipment artifacts although an alternative explanation has been proposed [16].

For the sample of pure copper (Figure 2) in an electrolyte containing no nickel ions the Nyquist plot consists of the resistance of the electrolyte, a semi circle due to the double layer and part of a second larger semi circle attributed to the passivation layer on the surface of the electrode. This is typical of a passivating sample where the passivation layer consists of only one phase. Two semicircles, one of which exhibits an inversion is a characteristic of a two layers passivation case.

From the Bode plot, Figure 2, it can be seen that as the nickel ion concentration increases the capacitance of the passive layer decreases slightly for additions of 10, 20, 30 g l^{-1} Ni^{2+}, and substantially when 40 g l^{-1} Ni^{2+} is added. This could be due to the passivation layer becoming either more porous or thicker.

As nickel ions are added to the electrolyte (Figure 2, 10 g l^{-1} Ni^{2+}) the Nyquist plot has same shape and indicates an increase in the ohmic resistance of the electrolyte as expected.

As the nickel content in the electrolyte increases to 20 g l^{-1} so does the ohmic resistance of the electrolyte, which agrees with previous findings [9]. The passivation layer still consists of one phase as indicated on the Nyquist plot.

As the nickel ion concentration is increased to 30 g l^{-1}, the Nyquist plot consists of the ohmic resistance of the electrolyte, a semi circle as the result of the double layer presence, an inverted loop, and part of a semi circle due to the passive layer presence. The inverted loop, characterized by an initial drop followed by a sudden rise in the imaginary part of the impedance, has been associated with the formation of a second phase in the passivation layer [17]. The capacitance of the layer changed by a small amount indicating, that the nature of the passive layer changed. This is most likely due to the precipitation of the second phase, which might make the passivation layer thicker and change its dielectric constant, thus changing its capacitance.

With the nickel ion concentration increasing to 40 g l^{-1}, the Nyquist plot consists of the ohmic resistance of the electrolyte, a semi circle caused by the double layer presence, an inverted loop, and part of a semi circle due to the presence of the passivation layer. It can be seen that the ohmic resistance did increase, which is in accordance to previous findings [9]. The passivation layer consists of two phases, as indicated by the inverted loop in Figure 2.

X-ray diffraction was used to identify the potential second phase. The XRD major peaks and the relative intensities of the compounds which may be expected on

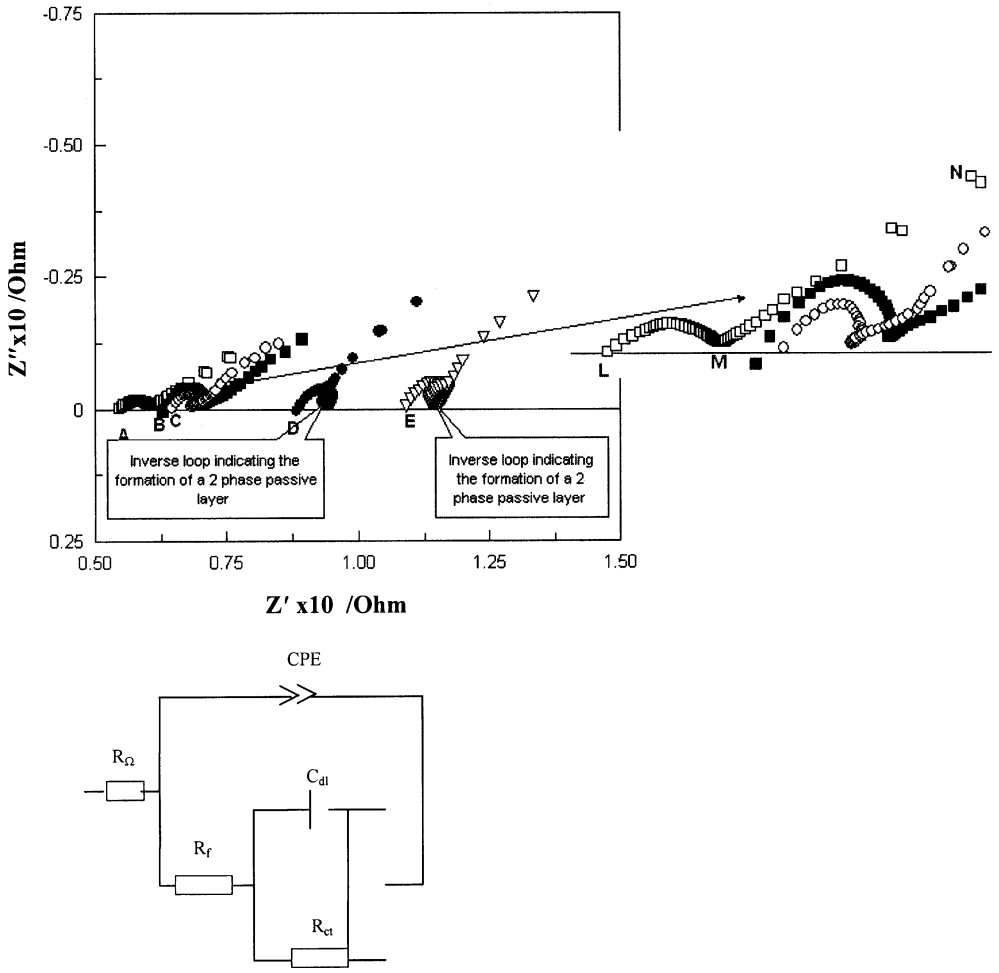

Fig. 2. Nyquist plot and the electrical equivalent circuit of a pure copper anode passivated in an electrolyte containing 160 g l^{-1} H_2SO_4, 40 g l^{-1} Cu^{2+} and 0, 10, 20, 30 or 40 g l^{-1} Ni^{2+}, at a bath temperature of 60 °C. (AC = 10 mV, Frequency from 10000 to 0.1 Hz, □ 0 g l^{-1} Ni^{2+}, ■ 10 g l^{-1} Ni^{2+}, ○ 20 g l^{-1} Ni^{2+}, ● 30 g l^{-1} Ni^{2+}, ▽ 40 g l^{-1} Ni^{2+}).

the surface of the passivated anodes are given in Table 3.

Figure 3 shows the intensity count vs 2-theta diffraction angle for a sample of a pure copper anode which was passivated in an electrolyte containing 160 g l^{-1} H_2SO_4, 40 g l^{-1} Cu^{2+} and 0 g l^{-1} Ni^{2+} at a bath temperature of 60 °C. It can be seen that major peaks, attributed to Cu_2O and CuO, appear at 42.29 and 89.76 degrees 2-theta, respectively. Therefore it seems that during this scan Cu_2O was formed and some of it transformed into CuO which is seen on the surface of the electrode. The same conclusion was also drawn from the CV plots [14].

Figure 4 shows the X-Ray spectrum of a pure copper anode passivated in an electrolyte containing 160 g l^{-1} H_2SO_4, 40 g l^{-1} Cu^{2+} and 10 g l^{-1} Ni^{2+}. The presence of $CuSO_4 \cdot 5H_2O$ was confirmed by the peaks that appear at 2-theta diffraction lines of 8.49,16.16 and 17. Only one peak, at 13.91 2-theta degree, attributed to the precipitation of $NiSO_4$ can be observed. A possible explanation is that after the formation of Cu_2O and CuO as was also indicated from the cyclic voltammetry experiments [14] a considerably thick layer of $CuSO_4 \cdot 5H_2O$ and $NiSO_4 \cdot 6H_2O$ either precipitated or electrochemically formed on the surface. Similar XRD spectra were observed for anode samples containing 1, 2, 3, 4, 5, and 6 w% nickel.

Table 3. Major 2θ peaks and their relative intensities in [ ] for compounds related to passivation of copper and copper/nickel alloys

Compound	2-θ (Relative Intensity)				
Cu (hkl)	43.29 [100] (111)	50.43 [46] (200)	74.13 [20] (220)	89.93 [17] (311)	116.92 [3] (400)
Cu_2O (hkl)	36.41 [100] (111)	42.29 [37] (200)	61.34 [27] (220)	73.52 [17] (311)	107.62 [3] (420)
CuO (hkl)	48.76 [25] (−202)	51.34 [2] (112)	72.41 [7] (311)	89.76 [6] (−131)	99.75 [4] (313)
$NiSO_4$ (hkl)	54.61 [8] (310)				
$CuSO_4 \cdot 5H_2O$ (hkl)	8.495 [5] (010)	16.16 [55] (−110)	17.00 [9] (020)	25.13 [20] (120)	26.99 [60] (−2−11)
$NiSO_4 \cdot 6H_2O$ (hkl)	13.91 [8] (101)	50.70 [2] (323)			

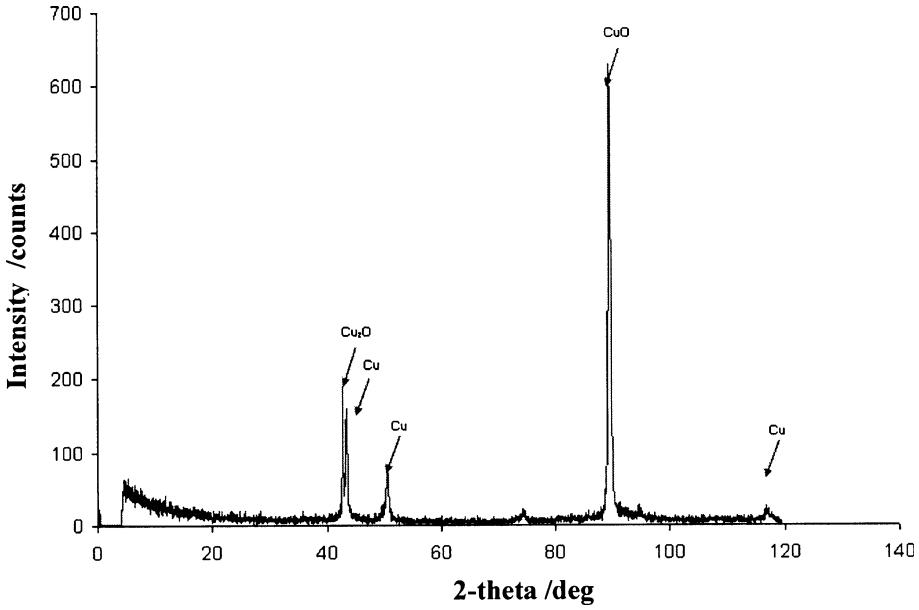

Fig. 3. XRD spectrum of a pure copper anode passivated in an electrolyte containing 160 g l^{-1} H_2SO_4, 40 g l^{-1} Cu^{2+} and 0 g l^{-1} Ni^{2+} at a bath temperature of 60 °C.

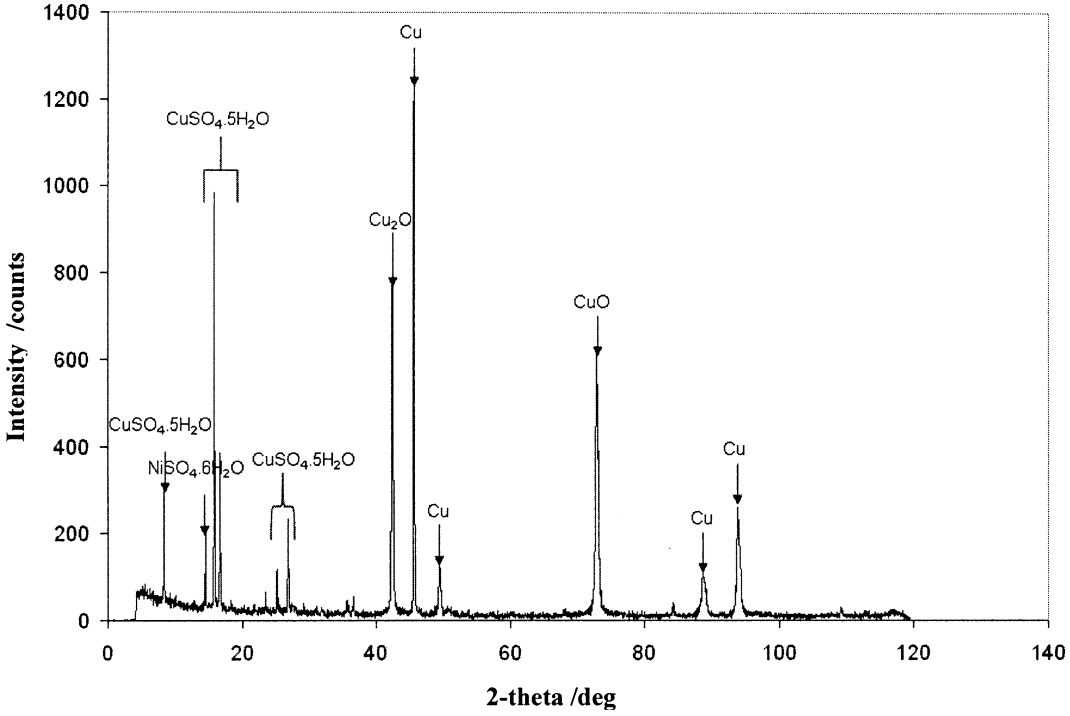

Fig. 4. XRD spectrum of a pure copper anode passivated in an electrolyte containing 160 g l^{-1} H_2SO_4, 40 g l^{-1} Cu^{2+} and 10 g l^{-1} Ni^{2+} at a bath temperature of 60 °C.

The diagrams in Figure 2 were fitted by the equivalent circuit of Figure 2. It can be seen that the electrolyte is represented by a resistor R_Ω. The double layer is represented as a capacitor, C_{dl}, in parallel with a charge transfer resistor, R_{CT}, and the passive layer is represented by a constant phase element CPE the impedance of which can be expressed in terms of CPE_T and CPE_P in the following manner [18, 19]:

$$Z_{CPE} = \frac{1}{CPE_T(j\omega)^{CPE_P}} \quad (5)$$

where CPE_T is the capacity of a constant phase element and CPE_P is a constant.

CPE_P generally has a value between −1 and 1, and CPE_T is the effective capacity of the CPE.

The results of correlation of experimental data with this equivalent circuit are given in Table 4 (a).

As the nickel ion concentration in the electrolyte increases from 0 to 40 g l^{-1} the CPE_P increases from 0.458 to 0.745 whereas no trend was observed between the changes in the CPE_T and the increase in the nickel ion concentration. When the nickel ion concentration in the electrolyte is 30 g l^{-1}, CPE_T has the lowest values compared to the other Ni^{2+} concentrations. A change in the CPE_T can be related to a change in the dielectric properties of the passivation layer as well as to a change in its area.

Nyquist and Bode plots for unrefined commercial copper anodes in an electrolyte containing 160 g l^{-1} H_2SO_4, 40 g l^{-1} Cu^{2+} and 0 and 40 g l^{-1} Ni^{2+}, were similar in appearance to the diagrams obtained for the pure copper anode in an electrolyte containing 0 and 40 g l^{-1} Ni^{2+}. Similar results were reported [10] but for a different frequency range. The results of correlation of experimental data for the unrefined copper anode with equivalent circuit of Figure 2 are given in Table 4 (b). There is a considerable increase in the values of R_Ω and CPE_P for the electrolytes containing 0 and 40 g l^{-1} Ni^{2+}, where a decrease in the CPE_T was observed for the electrolytes containing 0 and 40 g l^{-1} Ni^{2+}. The increase in R_Ω is due to the large amounts of impurities dissolving from the commercial anode.

Table 4. Equivalent circuit parameters for the passive surface, R_Ω, CPE_T and CPE_P for (a) pure copper anode, (b) commercial copper anode

Ni^{2+} concentration/g l^{-1}	R_Ω/Ω	$CPE_T/\mu F$	CPE_P
a			
0	5.5923	8.459	0.458
10	6.3683	6.87	0.493
20	6.4708	7.704	0.548
30	6.4708	5.986	0.709
40	8.8369	7.117	0.745
b			
0	6.504	10.28	0.801
40	10.04	9.291	0.917

The morphology of the various precipitation and passivation layers on the anodes was studied using a Cold Field Emission Electron Microscope. The nature of the layer seems to be very dependent on the nickel content of the electrolyte as well as the nickel content of the electrodes. Figure 5 shows the morphology of the passivation layer that formed on a pure copper anode that was passivated in an electrolyte containing 160 g H_2SO_4, 40 g l^{-1} Cu^{2+} and 0 g l^{-1} Ni^{2+} at a bath temperature of 60 °C. It can be seen that the layer has a good integrity. It consists mainly of CuO as determined by EDS. The high reflectivity $CuSO_4 \cdot 5H_2O$, seen on the surface of the layer, is the result of precipitation and was noted in the XRD spectra in Figure 4.

Figure 6 shows the Nyquist plots for a pure copper anode and copper anodes containing 1, 2, 3, 4, 5 and 6 w% nickel in an electrolyte containing 160 g l^{-1} H_2SO_4, 40 g l^{-1} Cu^{2+} and 0 g l^{-1} Ni^{2+}. The appearance of the reverse loop has been attributed to the formation of $CuSO_4$ whereas the disappearance of the reverse loop from the plots is due to $CuSO_4$ precipitating. As the nickel content in the electrodes increases, the ohmic resistance of the electrolyte changes as a result of nickel ions dissolving from the electrode. However, no correlation between the amount of nickel in the electrode and the change in the resistance could be made. The decrease in the ohmic resistance of the electrolyte for nickel

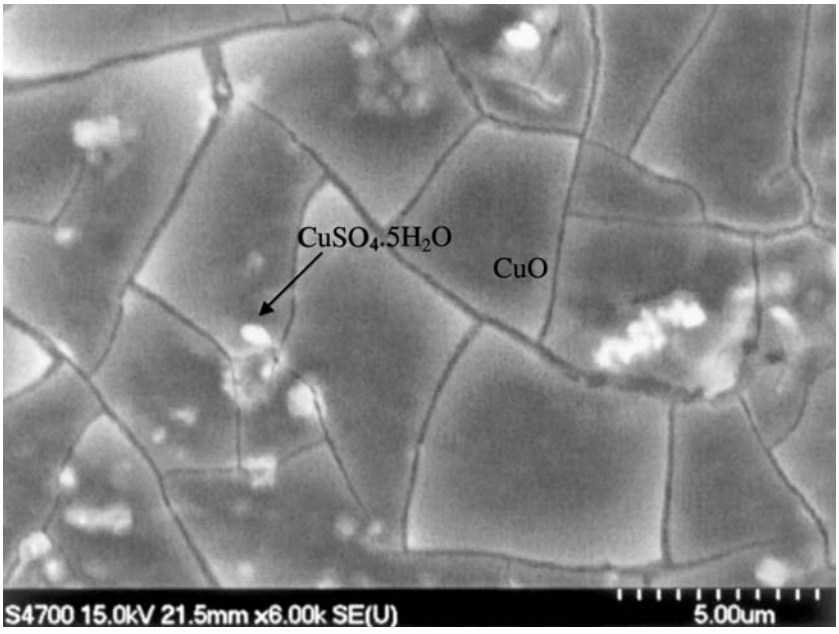

Fig. 5. SEM micrograph of the surface of a pure copper anode passivated in an electrolyte containing 160 g l^{-1} H_2SO_4, 40 g l^{-1} Cu^{2+} and 0 g l^{-1} Ni^{2+} at a bath temperature of 60 °C. CuO and $CuSO_4 \cdot 5H_2O$ are identified by arrows.

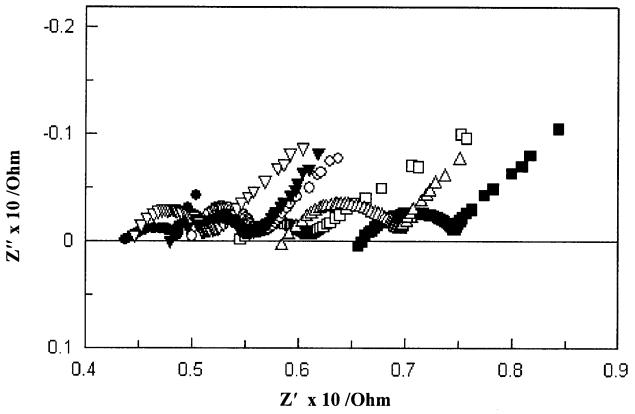

Fig. 6. Nyquist plot of a passivated copper anode containing 1, 2, 3, 4, 5, and 6 w% nickel in an electrolyte containing 160 g l^{-1} H_2SO_4, 40 g l^{-1} Cu^{2+} and 0 g l^{-1} Ni^{2+}, at a bath temperature of 60 °C. (AC = 10 mV, Frequency from 10 000 to 0.1 Hz, □ Pure copper, ■ Copper 1 w% nickel, ○ Copper 2 w% nickel, ● Copper 3 w% nickel, ▽ Copper 4 w% nickel, ▼ Copper 5 w% nickel, △ Copper 6 w% nickel).

addition of 2, 3, 4, and 5 w% nickel is not well understood and requires more study.

A change in the capacitance of the passivation layer can be seen with increasing nickel content in the electrode. But no correlation could be determined between the nickel content and the changes in the capacitance of the passivation layer.

All data generated for pure copper anodes and samples containing 1, 2, 3, 4, 5 and 6 w% nickel were fitted in circuits similar to the one shown in Figure 2. The results of correlation of experimental data with this equivalent circuit are given in Table 5. A change in the CPE_T occurs; this change could be due to changes in the area, the thickness and the dielectric properties of the passivation layer.

Figure 7 shows the Nyquist plot for a copper anode containing 2w% nickel in an electrolyte containing 160 g l^{-1} H_2SO_4, 40 g l^{-1} Cu^{2+} and 0, 10, 20, 30 or 40 g l^{-1} Ni^{2+}. Similarly to previous results (Figure 6) it can be seen that as the nickel ion concentration increases the ohmic resistance of the electrolyte increases which is in accordance with previous findings [9]. The passivation layer consisted of one phase with very similar capacitances. This is also reflected in the XRD spectra of both samples. The $CuSO_4 \cdot 5H_2O$ and $NiSO_4 \cdot 6H_2O$ detected in Figure 4 are a result of precipitation and not electrochemical formation, as indicated by the absence of the inverse loop on the Nyquist plot in Figure 7.

Table 5. Equivalent circuit parameters for the passive surface, R_Ω, CPE_T and CPE_P for synthetic copper/nickel anodes in 0 g l^{-1} nickel.

Nickel content/%w	R_Ω/Ω	$CPE_T/\mu F$	CPE_P
0	5.5923	8.459	0.458
1	6.6013	10.57	0.545
2	5.0035	11.66	0.511
3	6.0733	8.22	0.559
4	4.4639	10.29	0.481
5	4.7931	11.9	0.473
6	5.843	14.73	0.645

For a 20 g l^{-1} Ni^{2+} addition in the electrolyte, an increase in the ohmic resistance as well as a passivation layer consisting of two phases are observed. A significant drop in the capacitance of the passivation layer takes place, indicating a change in the dielectric property and/or layer thickness as well as the layer area. This drop is due, as indicated on the XRD spectrum (Figure 8), to the formation and precipitation of both $CuSO_4 \cdot 5H_2O$ and $NiSO_4 \cdot 6H_2O$ on the surface of the already formed passivation layer which consists of a mixture of CuO and Cu_2O.

As the nickel ion concentration increases to 30 g l^{-1}, a drop is observed in the ohmic resistance of the electrolyte; this anomalous behaviour which, was also observed in LSV, CP and CV [14] and it was attributed to precipitation. It can also be seen that the passivation layer consists of two phases, which is expected due to the presence of a high concentration of nickel ions in the electrolyte. An increase in the capacitance of the passivation layer could be due to the passivation layer being more porous, hence increasing its area which will lead to an increase in the capacitance.

The anomalous behaviour observed at a 30 g l^{-1} nickel ion concentration returns to normal when the concentration is increased to 40 g l^{-1}. At this concentration it can be observed from Figure 7 that the ohmic resistance of the electrolyte increases and that the passivation layer consists of two phases, which is indicated by the presence of the inverse loop on the curve E.

The capacitance of the passivation layer decreases, which is probably the result of an increase in its thickness due to the formation and the precipitation of $CuSO_4 \cdot 5H_2O$ and $NiSO_4 \cdot 6H_2O$ as seen from the XRD spectrum of Figure 8. The morphology of this passivation layer is given in Figure 9. The $CuSO_4 \cdot 5H_2O$ that exists on the surface of the layer is different than that

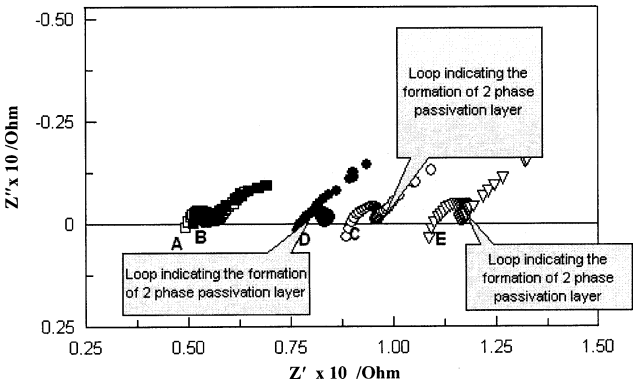

Fig. 7. Nyquist plot of a copper anode containing 2 w% nickel passivated in an electrolyte containing 160 g l^{-1} H_2SO_4, 40 g l^{-1} Cu^{2+} and 0, 10, 20, 30, or 40 g l^{-1} Ni^{2+}, at a bath temperature of 60 °C. (AC = 10 mV, Frequency from 10 000 to 0.1 Hz, A: □ 0 g l^{-1} nickel ions, B: ■ 10 g l^{-1} nickel ions, C: ○ 20 g l^{-1} nickel ions, D: ● 30 g l^{-1} nickel ion and E: ▽ 40 g l^{-1} nickel ions).

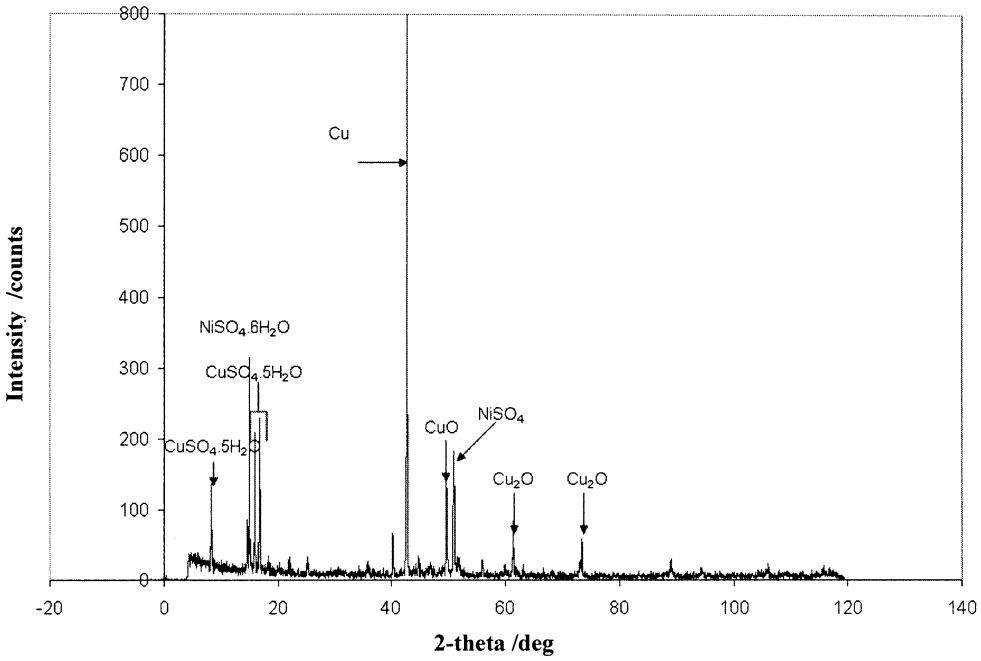

Fig. 8. XRD spectrum of a pure copper anode passivated in an electrolyte containing 160 g l^{-1} H_2SO_4, 40 g l^{-1} Cu^{2+} and 20 g l^{-1} Ni^{2+} at a bath temperature of 60 °C.

precipitated on the layers formed in electrolytes containing no nickel ions and 10 g l^{-1} Ni^{2+}. This suggests that the $CuSO_4 \cdot 5H_2O$ on the present layer formed electrochemically, which is in agreement with the results seen in EIS suggesting that the layer contains a minimum of two phases. The passivation layer consists mainly of CuO.

Figure 10 shows the Nyquist plot for a copper anode containing 4w% nickel in an electrolyte containing 160 g l^{-1} H_2SO_4, 40 g l^{-1} Cu^{2+} and 0, 10, 20, 30 or 40 g l^{-1} Ni^{2+}. This sample was chosen to illustrate the additions of Ni content on the anode on the passivation.

For nickel addition of 10 g l^{-1} Ni^{2+} the ohmic resistance increases substantially and the passivation layer consists of only one phase with a capacitance lower than the capacitance of the passivation layer formed on the sample in an electrolyte that does not contain any nickel ions. Such behaviour may be attributed to a change in the porosity of the passivation layer, its roughness or thickness. Also as seen from the XRD of Figure 8, $NiSO_4 \cdot 6H_2O$ and $CuSO_4 \cdot 5H_2O$ formed on the surface of the passivation layer. All these possible changes might lead to a porous layer which causes the decrease in its capacitance.

Similar behaviour was observed for an addition of 20 g l^{-1} Ni^{2+} in the electrolyte. As the nickel ion concentration is increased to 30 g l^{-1} Ni^{2+}, the Nyquist plot indicates that the passivation layer consists of a minimum of two phases, which have a lower capacitance than the layers formed in the electrolytes containing 0, 10 and 20 g l^{-1} Ni^{2+}. This behaviour is expected since the passive layer consists of a minimum of one extra phase, which is indicated by the presence of the inverse loop on curve "D" in Figure 10 and could be due to the substantial amount of nickel ion dissolving from the electrode in the electrolyte. This causes a rapid increase in the nickel ion concentration in the vicinity of the surface of the electrode causing $NiSO_4 \cdot 6H_2O$ or $CuSO_4 \cdot 5H_2O$ to precipitate and insulate the surface.

As the nickel ion concentration is increased to 40 g l^{-1} the passivation layer no longer consists of several electrochemically formed phases but only one phase.

Figure 11 shows the Nyquist plot for a copper anode containing 6w% nickel in an electrolyte containing 160 g l^{-1} H_2SO_4, 40 g l^{-1} Cu^{2+} and 0, 10, 20, 30 or 40 g l^{-1} Ni^{2+}.

For a sample of copper that contains 6 w% nickel, the presence of inverse loops leads to the interpretation that a passivation layer consisting of a minimum of two phases is formed for nickel concentrations of 20 and 30 g l^{-1}.

As the nickel ion concentration increases to 40 g l^{-1} the passivation layer consists of a single phase as indicated by the absence of the inverse loop.

To illustrate the effect of Ni in the Cu anode and Ni^{2+} in the electrolyte, Figure 12 shows the morphology of the passivation layer formed on a copper anode containing 6 w% nickel passivated in electrolyte containing 40 g l^{-1} Ni^{2+} at 60 °C. The $CuSO_4 \cdot 5H_2O$ on the surface of the layer again has a different structure than that precipitated on the layers formed in electrolytes containing no nickel ions and 10 g l^{-1} Ni^{2+}. The $CuSO_4 \cdot 5H_2O$ precipitates are round and dull looking suggesting that the $CuSO_4 \cdot 5H_2O$ formed electrochemically, which is in agreement with the EIS results, suggesting that the layer formed on the copper anode containing 6 w% nickel consists of a minimum of two phases. The inner passivation layer still consists mainly of CuO and

Fig. 9. SEM micrograph of the surface of a copper anode containing 2 w% Ni passivated in an electrolyte containing 160 g l^{-1} H_2SO_4, 40 g l^{-1} Cu^{2+} and 40 g l^{-1} Ni^{2+} at a bath temperature of 60 °C. CuO, $CuSO_4 \cdot 5H_2O$ and $NiSO_4 \cdot 6H_2O$ are indicated by arrows.

the $NiSO_4 \cdot 6H_2O$ seen is similar to that formed previously in Figure 9.

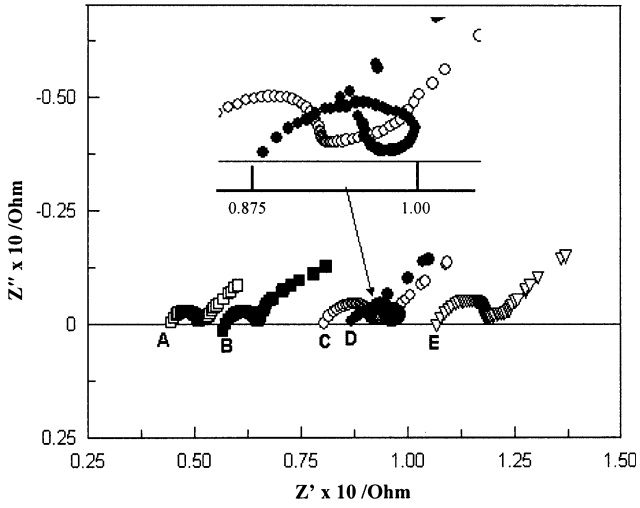

Fig. 10. Nyquist plot of a copper anode containing 4 w% nickel passivated in an electrolyte containing 160 g l^{-1} H_2SO_4, 40 g l^{-1} Cu^{2+} and 0, 10, 20, 30, or 40 g l^{-1} Ni^{2+}, at a bath temperature of 60 °C. (AC = 10 mV, Frequency from 10 000 to 0.1 Hz, A: □ 0 g l^{-1} nickel ions, B: ■10 g l^{-1} nickel ions, C: ○ 20 g l^{-1} nickel ions, D: ● 30 g l^{-1} nickel ion and E: ▽ 40 g l^{-1} nickel ions).

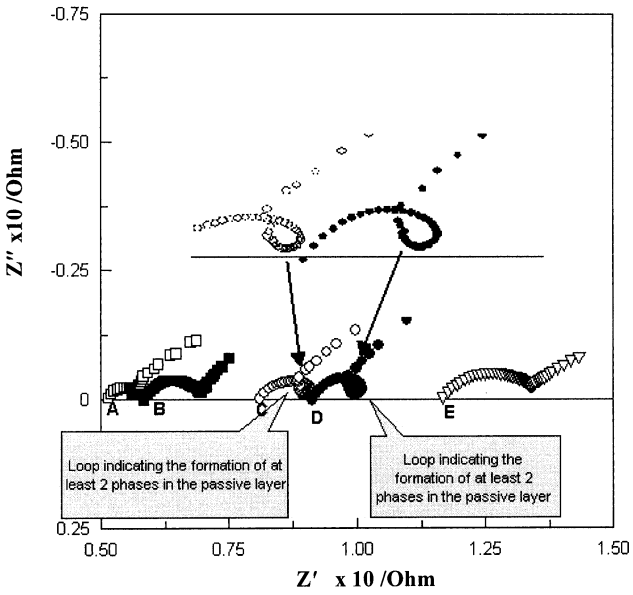

Fig. 11. (a) Nyquist plot of a copper anode containing 6 w% nickel passivated in an electrolyte containing 160 g l^{-1} H_2SO_4, 40 g l^{-1} Cu^{2+} and 0, 10, 20, 30, or 40 g l^{-1} Ni^{2+}, at a bath temperature of 60 °C. (AC = 10 mV, Frequency from 10 000 to 0.1 Hz, A: □ 0 g l^{-1} nickel ions, B: ■ 10 g l^{-1} nickel ions, C: ○ 20 g l^{-1} nickel ions, D: ● 30 g l^{-1} nickel ion and E: ▽ 40 g l^{-1} nickel ions).

5. Conclusions

From EIS experiments it is concluded that nickel ion additions to the electrolyte increased the resistance of the electrolyte, R_Ω. It is also concluded that the porosity, thickness and constituents of the passivation layer changed with nickel ion addition to the electrolyte. The circuit models generated from the data acquired during EIS experiments calculated values for the electrical components consistent with these conclusions. EIS experiments on samples prepared from an unrefined commercial clipper anode followed the same behaviour as the synthetically prepared samples thus indicating that the conclusions above also applied to commercial unrefined anodes.

Additions of nickel to the electrolyte, as well as to the electrode, had an effect on the electrical properties of the

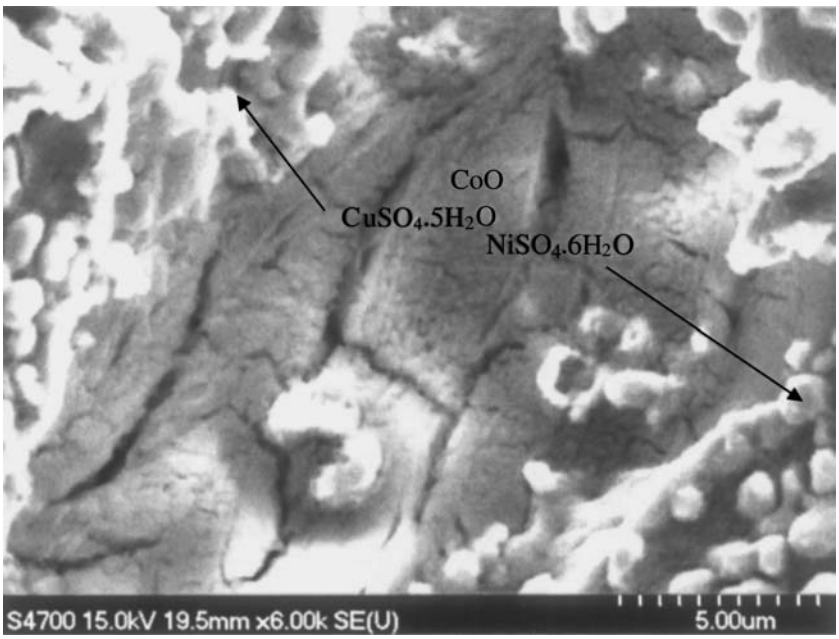

Fig. 12. SEM micrograph of the surface of a copper anode containing 6 w% Ni passivated in an electrolyte containing 160 g l^{-1} H_2SO_4, 40 g l^{-1} Cu^{2+} and 40 g l^{-1} Ni^{2+} at a bath temperature of 60 °C. CuO, $CuSO_4 \cdot 5H_2O$ and $NiSO_4 \cdot 6H_2O$ are indicated by arrows.

passivation layer as calculated from the corresponding equivalent circuits. However, this effect was more pronounced when nickel was added to the electrolyte than when it was added to the electrode.

Scanning Electron Microscopy revealed when the nickel ion concentration in the electrolyte increased, there was an increase in the amount of precipitated $CuSO_4 \cdot 5H_2O$ and $NiSO_4 \cdot 6H_2O$ on the surface of the oxide layer. Nickel additions to the anode did not have a noticeable effect on the amount of precipitate on the surface of the oxide layer but had a definite effect on its structure. As the nickel content increased in the anodes the oxide layer appeared more porous and had a layered structure. As a result it would be expected that an increase in the nickel content in the anode causes the passive layer to become less stable and be less effective in slowing electron transport.

Acknowledgements

The authors thank Dr. Jeff Dahn for allowing use of the FRA equipment. The financial assistance of the Natural Sciences and Engineering Research Council of Canada (NSERC) and the Atlantic Innovation Fund (AIF) is gratefully acknowledged.

References

1. A.K. Biswas and W.G. Davenport, *Extractive Metallurgy of Copper*, 2nd edn., (Pergamon Press, London, 1980), pp. 230–238.
2. S. Abe, B. Burrows and V.A. Ettel, *Can. Metall. Quart.* **19** (1980) 289.
3. S. Jin, E. Ghali and A. Adnot, AES Study on The Passivation Mechanism of Copper Anodes Electrolyzed in H_2SO_4-$CuSO_4$ Solution, Report AES, Laval University, (1991).
4. T.T. Chen and J.E. Dutrizac, *JOM* **56** (2004) 48.
5. M. Girgis and E. Ghali, ''Electrochemical Investigations on the Behavior of Arsenic During Copper Electrodeposition'', Report AES, Laval University, (1985).
6. Y. Konishi, Y. Tanaka, Y. Kondo and Y. Fukunaka, *Electrochim. Acta* **46** (2000) 681.
7. Y. Konishi, Y. Nakamura, Y. Fukunaka, K. Tsukada and K. Hanasaki, *Electrochim. Acta* **48** (2003) 2615.
8. M Muinonen, G. Jarjoura and G.J. Kipouros, *in* Effect of Nickel Impurity and Temperature on the Diffusion Coefficient of Copper Ions in a Copper Sulphate Solution, The International Terje Ostvold Symposium, H.A. Oye and O. Waernes, (eds). (Trondheim, Norway, 1998) 105.
9. G. Jarjoura, M. Muinonen and G.J. Kipouros, *Can. Metall. Quart.* **42** (2003) 281.
10. M.S. Moats and J.B. Hiskey, *Can. Metall. Quart.* **39** (2000) 297.
11. X. Cheng and J.B. Hiskey, *Metall. Mater. Trans. B* **27B** (1996) l.
12. X. Cheng and J.B. Hiskey, *Metall. Mater. Trans. B* **27B** (1996) 610.
13. J.B. Hiskey and X. Cheng, *Metall. Mater. trans. B* **29B** (1998) 53.
14. G. Jarjoura, Electrochemical Investigation of Copper/Nickel Alloys in Copper Sulfate Solution Containing Nickel Using LSV, CP, CV, and EIS, Ph.D. Thesis (Dalhousie University, Halifax, Nova Scotia, Canada 2004).
15. G.J. Kipouros, R.N. Seefurth and R.A. Sharma, *in* S.K. Das, (Ed.), Light Metals 1993, (TMS/AIME, Warrendale, PA, 1993) 1105.
16. B. Bozzini, C. Mele and L. Sgura, *J. Appl. Electrochem.* **34** (2004) 277.
17. E.P. Grishina, A.M. Udalova and E.M. Rumyantsev, *Russ J. Electrochem.* **38**(9) (2002) 1041.
18. A. Bard and L. Faulkner, *Electrochemical Methods Fundamentals and Applications* (John Wiley & Sons, Toronto, 1980), pp. 27.
19. C. Gabrielli, Identification of Electrochemical Processes by Frequency Response Analysis, Technical Report, August 1984.